https://doi.org/10.7770/jonraf-v2-art2905

JONRAF Journal of Natural Resources and Farming

SPECIAL ISSUE

Proportional discrete Fourier analysis of WaPOR actual evapotranspiration and interception over cropland in Comayagua, Honduras

Carlos M. Cruz-Rodas[a*], Marlon M. López-Flores[b], William Campillay-Llanos[c,d]

Master's Program in Mathematics, National Autonomous University of Honduras, Tegucigalpa[a], Honduras
Artificial Intelligence, Robotics and Cybernetics Laboratory (LIARC), Military Institute of Engineering (IME-RJ), Rio de Janeiro[b], Brazil
Department of Mathematical and Physical Sciences, Catholic University of Temuco, Temuco[c], Chile
Research Center for Food Production, Catholic University of Temuco, Temuco[d], Chile

Article history
Received: 10/02/2026
Accepted: 20/07/2026
Published: 22/09/2026

Corresponding author
*Carlos M. Cruz-Rodas
carlos.cruz@unah.edu.hn

ABSTRACT
Purpose: Positive agronomic variables are often interpreted using ratios and relative seasonal contrasts. This study examines whether annual seasonality remains dominant when WaPOR actual evapotranspiration and interception (AETI) is centered proportionally rather than additively. **Methods:** A monthly series was extracted for January 2018–December 2025 from cropland-screened WaPOR version 3 Level 1 cells within Comayagua, Honduras. The screen combined the Food and Agriculture Organization (FAO) Global Administrative Unit Layers (GAUL) 2015 first-level boundary with European Space Agency (ESA) WorldCover 2021 class 40. For each month, dekadal values were averaged with equal weight within each cell, after which the spatial median was calculated across 1,094 valid WaPOR cells. A representative proportional spectrum was computed as the unitary discrete Fourier transform of the centered logarithmic series and compared with the transform of the centered original series. **Results:** All 96 monthly observations were strictly positive. The geometric mean was 2.4571 mm day^{-1}. The dominant proportional coefficient occurred at $k = 8$, the annual bin, with; the semiannual coefficient was $A_p(16) = 0.5252$. These bins accounted for 72.41% and 10.88% of one-sided proportional power. The direct spectrum was also dominated by $k = 8$. **Conclusions:** Proportional spectral analysis provides a unit-invariant characterization of relative AETI variability. It does not represent a different Fourier algorithm, but it distinguishes multiplicative deviations from absolute water-flux amplitudes.

Keywords: proportional arithmetic; spectral seasonality; WaPOR; crop water use; remote sensing; relative variability

1. Introduction

Actual evapotranspiration is central to crop-water assessment because it links atmospheric demand, vegetation response, and water consumption (Allen et al. 1998). Many related natural-resource variables are strictly positive and are interpreted through ratios, elasticities, or percentage changes. For such variables, the same absolute change can have different meanings at different baselines. A relative spectral interpretation may therefore complement the conventional spectrum when the comparison concerns seasonal contrast rather than absolute water flux.

Classical Fourier analysis detects periodic structure by decomposing additive variation. If a process is naturally described by multiplicative fluctuations, analyzing the original scale can mix the baseline magnitude with relative oscillations. Taking logarithms converts ratios into differences, but proportional arithmetic gives this operation a structural interpretation: proportional addition is multiplication and proportional subtraction is division. This framework belongs to the broader family of non-Newtonian and non-Diophantine arithmetics transported through bijections (Grossman and Katz 1972; Burgin and Czachor 2020; Czachor 2020). Its positive-real realization is connected with multiplicative and proportional calculus (Bashirov et al. 2008; Pinto et al. 2020; Campillay-Llanos et al. 2021). It is also related, but not identical, to Mellin analysis on the multiplicative half-line (Butzer and Jansche 1997; Folland 1995).

This distinction should be stated carefully. The computation developed below is an ordinary discrete Fourier transform in logarithmic representative coordinates. The proportional contribution lies in the transported arithmetic, geometric centering, scale invariance, and coefficient interpretation. It is not an unrelated fast transform and does not replace Fourier or Mellin analysis.

The empirical application uses the Food and Agriculture Organization (FAO) WaPOR version 3 Level 1 AETI product. Each pixel represents average daily actual evapotranspiration and interception over a dekad, with a 0.1 scale factor and a nominal pixel size of approximately 248 m (FAO 2018, 2025; FAO WaPOR 2026). WaPOR products have been evaluated as operational evapotranspiration sources, although product-level validation does not replace local field validation (Blatchford et al. 2020). To avoid an arbitrary rectangular window, the present study screens WaPOR cells using European Space Agency (ESA) WorldCover 2021 cropland class 40 inside the FAO Global Administrative Unit Layers (GAUL) 2015 Comayagua boundary (FAO GAUL 2026; ESA WorldCover Consortium 2026; Zanaga et al. 2022).

The research question addressed in this study is whether annual seasonality dominates both relative and absolute variability in the resulting positive AETI series. The objective is to define a rigorous representative proportional DFT, apply it to the public Comayagua series, and compare annual and semiannual components with the direct DFT under the same unitary normalization.

2. Materials and Methods

2.1 Proportional centering and representative DFT

Let $\mathbb{R}_+ = (0,\infty)$ and let the logarithmic representative be

$$\mathcal{R}_p(x) = \ln x. \tag{1}$$

Transporting ordinary addition and subtraction through $\mathcal{R}_p$ gives

$$x \oplus y = xy, \qquad x \ominus y = \frac{x}{y}. \tag{2}$$

The proportional zero is 1. For a positive series $x = (x_0, \ldots, x_{N-1}) \in \mathbb{R}_+^N$, its proportional mean is the geometric mean

$$\bar{x}_p = \mathrm{gm}(x) = \exp\left(\frac{1}{N}\sum_{m=0}^{N-1} \ln x_m\right), \tag{3}$$

and proportional centering is

$$x_n^c = x_n \ominus \bar{x}_p = \frac{x_n}{\bar{x}_p}. \tag{4}$$

Hence

$$\widetilde{y}_n = \mathcal{R}_p(x_n^c) = \ln x_n - \frac{1}{N}\sum_{m=0}^{N-1} \ln x_m. \tag{5}$$

To compute the spectral coefficients, let $\mathbb{C}_p$ be the formal proportional copy of $\mathbb{C}$ and extend $\mathcal{R}_p$ componentwise from $\mathbb{C}_p$ to $\mathbb{C}$. The proportional DFT is then defined through this classical complex representative. With unitary normalization,

$$\mathcal{R}_p((\mathcal{D}_p x)_k) = \widehat{y}_k = \frac{1}{\sqrt{N}}\sum_{n=0}^{N-1} \widetilde{y}_n \exp\quad -2\pi i\frac{kn}{N} \quad, \qquad k = 0, \ldots, N-1. \tag{6}$$

All numerical coefficients reported in this paper are representative coefficients $\hat{y}_k$. Their amplitude and power are

$$A_p(k) = |\widehat{y}_k|, \qquad P_p(k) = |\widehat{y}_k|^2. \tag{7}$$

Since the normalization in equation (6) is unitary, Parseval's identity holds in representative coordinates:

$$\sum_{n=0}^{N-1} |\widetilde{y}_n|^2 = \sum_{k=0}^{N-1} |\widehat{y}_k|^2. \tag{8}$$

For the real series analyzed here, the one-sided power share is

$$S_p(k) = \frac{P_p(k)}{\sum_{j=1}^{N/2} P_p(j)}, \qquad 1 \le k \le N/2. \tag{9}$$

For comparison, the direct coefficients are

$$\widehat{x}_k = \frac{1}{\sqrt{N}}\sum_{n=0}^{N-1} (x_n - \bar{x}) \exp\quad -2\pi i\frac{kn}{N} \quad, \qquad A_d(k) = |\widehat{x}_k|. \tag{10}$$

The direct amplitude has the units of AETI, whereas $A_p(k)$ is the amplitude of a dimensionless log-ratio representative.

If $z_n = cx_n$ for $c > 0$, then centering eliminates ln c, and therefore

$$A_p^z(k) = A_p^x(k), \qquad P_p^z(k) = P_p^x(k). \tag{11}$$

Thus, the representative proportional spectrum is invariant under positive unit rescaling. For monthly observations, the period associated with index $k \neq 0$ is

$$T_k = \frac{N}{k} \quad \text{months.} \tag{12}$$

With $N = 96$, annual and semiannual cycles occur exactly at $k = 8$ and $k = 16$.

2.2 Study region and geospatial data

The study region was the first-level administrative unit of Comayagua, Honduras, from the FAO Global Administrative Unit Layers (GAUL) 2015 dataset. Cropland screening used ESA WorldCover 2021 v200 class 40 at 10 m resolution (FAO GAUL 2026; ESA WorldCover Consortium 2026; Zanaga et al. 2022). The screening layer corresponds to a publicly available land-cover classification rather than a field-validated crop inventory, an irrigation-district boundary, or a crop-specific map.

AETI was obtained from the public Earth Engine collection `FAO/WAPOR/3/L1_AETI_D`, band `L1-AETI-D`, for January 2018–December 2025. Catalog values were multiplied by 0.1. The WorldCover mask was evaluated on the WaPOR analysis grid at 250 m. Google Earth Engine uses nearest-neighbor resampling by default during reprojection; consequently, the resulting 1,094 valid cells are cropland-screened WaPOR cells rather than fractional cropland-area estimates (Google Earth Engine 2026). Figure 1 was prepared in QGIS 3.34.12 from the supplied GAUL, WorldCover, and OpenStreetMap layers (OpenStreetMap contributors 2026).

2.3 Monthly aggregation and reproducible spectral workflow

Let $s_{d,j}$ be the scaled WaPOR daily-rate value for dekad d and WaPOR cell j. For month n, the archived series was defined as

$$x_n = \mathrm{median}_{j\in\Omega}\left(\frac{1}{|M_n|}\sum_{d\in M_n} s_{d,j}\right), \tag{13}$$

where M_n contains the available dekadal images in month n and Ω is the cropland-screened set. Thus, each dekad received equal weight, and the spatial median was then calculated. The median reduces sensitivity to isolated cell anomalies. Only finite, strictly positive monthly values were retained. The archived table contained all 96 consecutive months, with 1,094 valid cells included in every monthly reduction.

Equal-dekad averaging is the estimand analyzed here. Because the final dekad contains 8–11 days depending on month, it is not identical to a day-weighted monthly daily rate. The supplementary Earth Engine script therefore exports both equal-dekad and day-weighted variants for sensitivity analysis. This distinction is reported explicitly as a limitation.

3. Results

The 96 monthly AETI observations ranged from 1.2333 to 3.5000 mm day^{-1}. The arithmetic mean was 2.5201 mm day^{-1} and the proportional mean was 2.4571 mm day^{-1}. Figure 2

Figure 1.

Study region and spatial screening used for the WaPOR extraction. Brown areas show ESA WorldCover 2021 class-40 cropland pixels within the red Comayagua boundary; black lines indicate first-level administrative boundaries. The inset shows the location of Comayagua within Honduras. Basemap: OpenStreetMap contributors; administrative boundary: FAO GAUL 2015; cropland class: ESA WorldCover 2021.

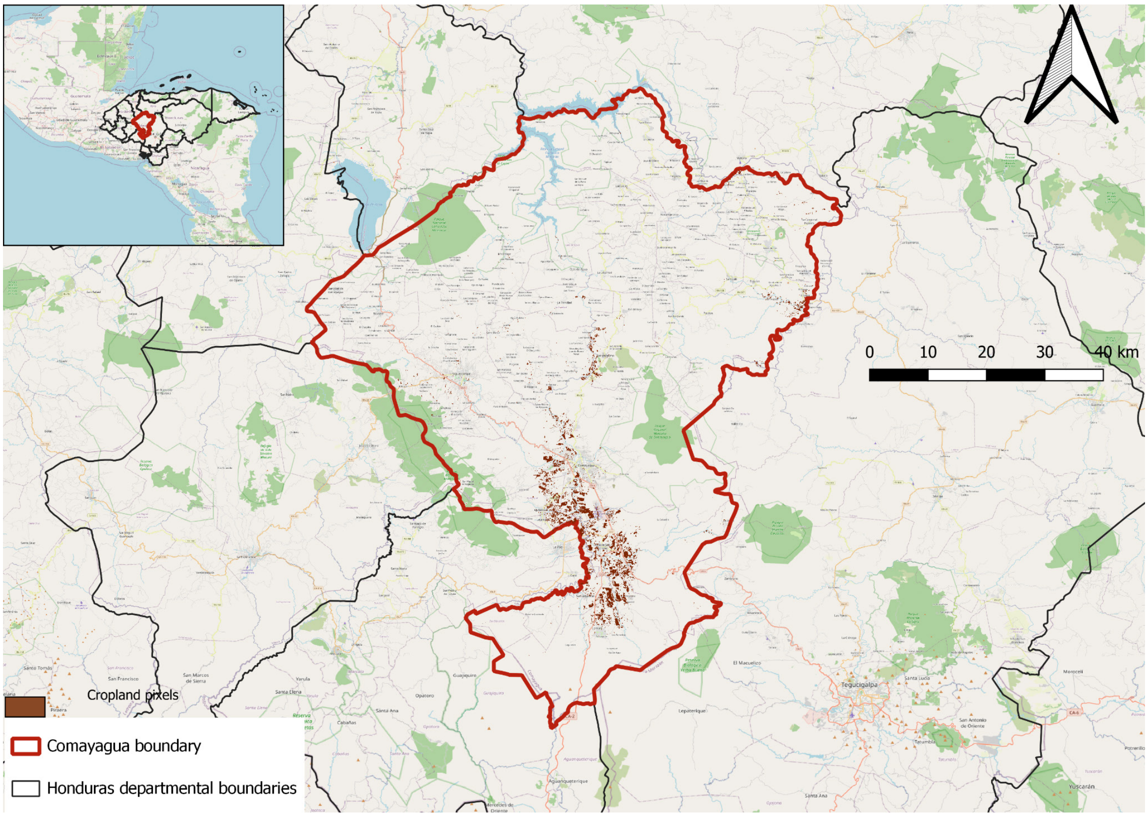

Figure 2.

Monthly WaPOR AETI over cropland-screened cells in Comayagua. Panel (a) shows AETI and the geometric-mean baseline. Panel (b) shows proportional centering as $x_n/\bar{x}_p$; the dashed line marks the proportional zero at 1.

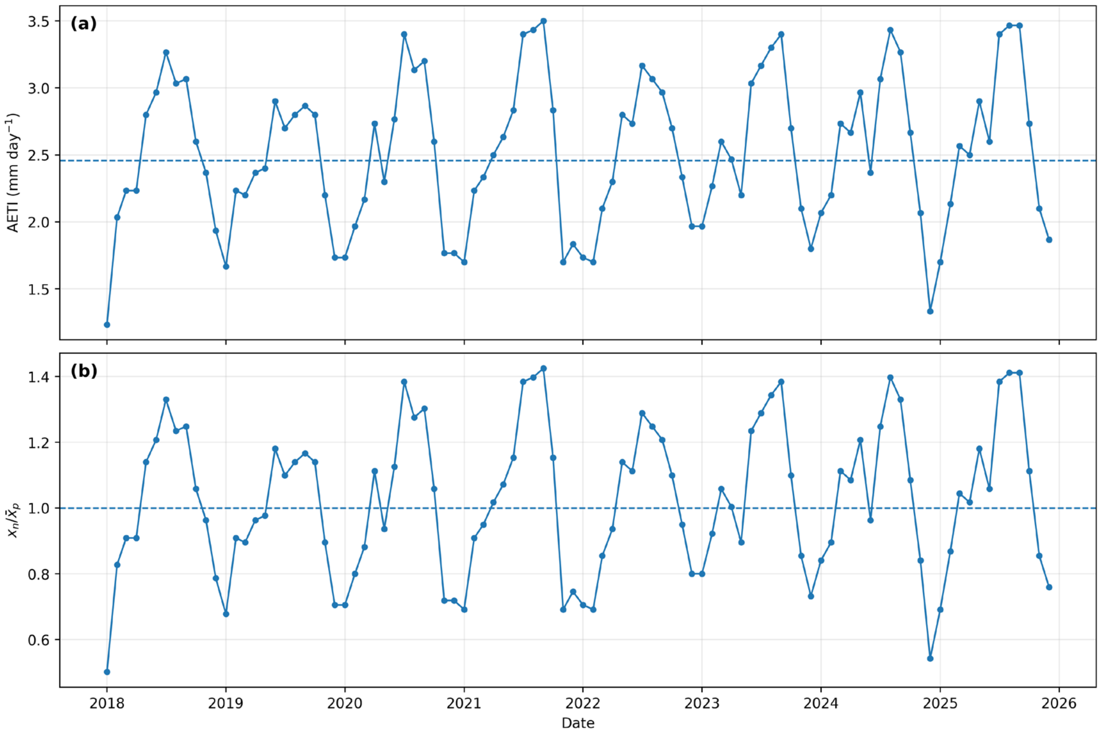

Figure 3.

One-sided discrete Fourier amplitudes. Panel (a) shows the representative proportional amplitude $A_p(k)$ of the centered logarithmic series. Panel (b) shows the direct amplitude $A_d(k)$ of the centered original series. Dashed and dotted lines mark the annual ($k = 8$) and semiannual ($k = 16$) bins.

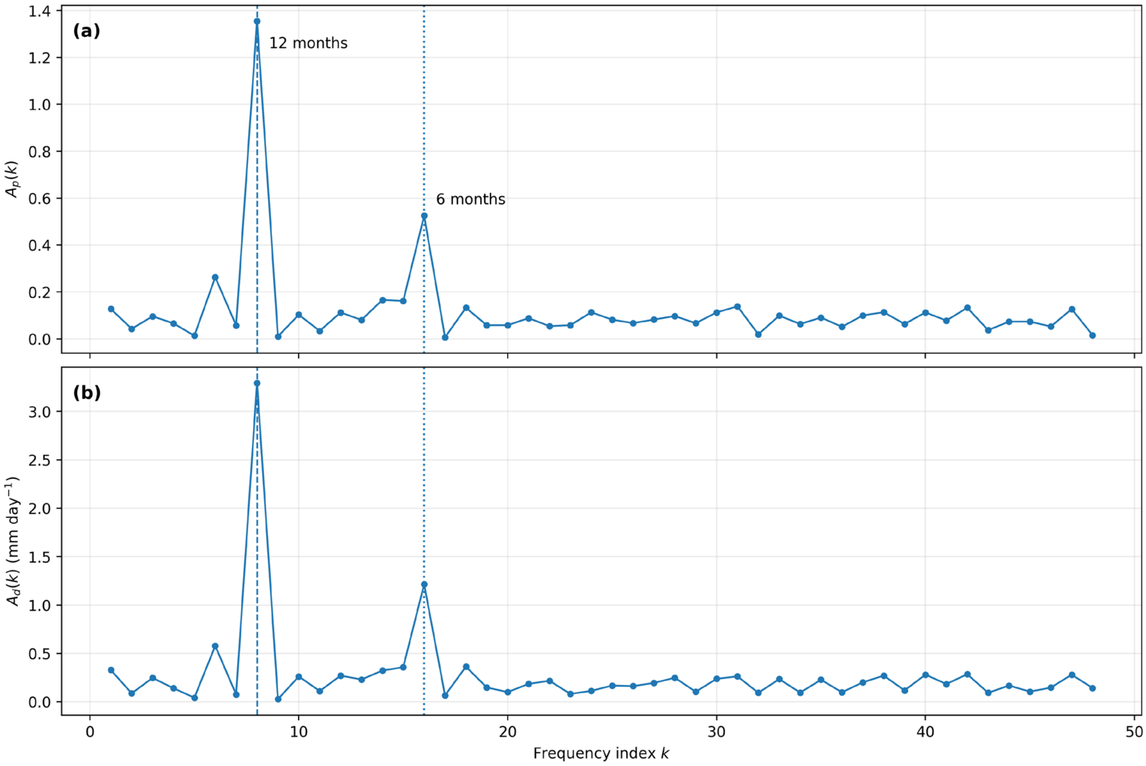

Table I

Empirical quantities for the proportional and direct WaPOR AETI spectra

Quantity	Value	Interpretation
Analysis window	2018-01–2025-12	Eight complete calendar years
Valid observations	$N = 96$	Consecutive monthly series
Valid cropland-screened cells	1,094	Constant monthly count
Arithmetic mean AETI	2.5201 mm day^{-1}	Ordinary baseline
Geometric mean AETI	2.4571 mm day^{-1}	Proportional baseline
Dominant proportional index	$k = 8$	12-month relative component
Annual proportional amplitude	$A_p(8) = 1.3549$	Log-ratio representative
Annual proportional power share	72.41%	One-sided nonzero power
Semiannual proportional amplitude	$A_p(16) = 0.5252$	6-month relative component
Semiannual proportional power share	10.88%	One-sided nonzero power
Annual direct amplitude	$A_d(8) = 3.2929$ mm day^{-1}	Absolute-amplitude component
Semiannual direct amplitude	$A_d(16) = 1.2139$ mm day^{-1}	Absolute-amplitude component

shows the original series and the centered ratio $x_n/\bar{x}_p$. Ratios greater than 1 indicate months above the geometric baseline; ratios below 1 represent months below it.

The dominant representative proportional amplitude occurred at k = 8, corresponding to 12 months. The annual amplitude was $A_p(8)$ = 1.3549 and the semiannual amplitude was $A_p(16)$ = 0.5252. Their one-sided power shares were 72.41% and 10.88%, respectively. The direct spectrum was also dominated by k = 8, with $A_d(8)$ = 3.2929 mm day^{-1} and Ad(16) = 1.2139 mm day^{-1}. The corresponding direct power shares were 74.88% and 10.18% (Table I, Fig. 3).

4. Discussion

The dominance of the same index in both spectra indicates strong annual seasonality in both relative and absolute terms for the extracted series. The interpretation differs, however. The direct coefficient measures absolute AETI variation, while the proportional coefficient measures oscillation of the log ratio around the geometric baseline. Scale invariance in equation (11) makes the latter suitable for comparisons under equivalent positive unit changes or multiplicative calibration factors.

These results are descriptive rather than causal. The annual peak alone cannot distinguish among rainfall seasonality, irrigation, crop calendars, phenology, and land-cover classification error. Similarly, the semiannual peak is a secondary spectral feature, not evidence of a specific double-cropping mechanism. Independent evaluations support the operational use of WaPOR products but also document product uncertainty; therefore, they do not validate the local mask or monthly aggregation used here (Blatchford et al. 2020).

Four limitations constrain the scope of this conclusion. First, a static 2021 land-cover class was applied across 2018–2025 and does not capture crop rotation or land-cover change. Second, nearest-neighbor screening on the coarser WaPOR grid does not estimate fractional cropland coverage and includes mixed cells. Third, equal-dekad monthly averaging differs slightly from day-weighted averaging in months with a shorter or longer final dekad. Fourth, DFT amplitudes depend on record length and normalization; cross-region amplitude comparisons should use a common N or compare normalized power shares. These limitations do not alter the arithmetic correspondence, but they restrict the agronomic generalizability of the findings.

5. Conclusions

The representative proportional DFT provides a coherent spectral interpretation for strictly positive agronomic series when the target is relative rather than absolute variability. It is obtained by dividing observations by their geometric mean, applying the logarithmic representative, and computing the ordinary unitary DFT. The calculation is therefore reproducible with standard Fourier routines, while the proportional interpretation remains explicit.

For the 96-month WaPOR AETI series over cropland-screened cells in Comayagua, the annual bin k = 8 dominated both the proportional and direct spectra. The proportional annual amplitude was 1.3549, accounting for 72.41% of one-sided proportional power, while the semiannual component was weaker. This finding supports the specific conclusion that annual relative seasonality dominates the analyzed public-data series.

The method is not a replacement for classical Fourier or Mellin analysis and does not establish crop-specific water requirements. Its practical value lies in distinguishing multiplicative seasonal contrast from absolute AETI amplitude. Field-validated crop boundaries, day-weighted monthly sensitivity analyses, precipitation and irrigation data, and crop calendars are needed before the results can inform management or policy decisions.

Declarations

Funding. M.M.L.-F. received partial funding from project EVAAT-GCN under FINEP agreement 01.24.0661.00, ref. 3311/24.

Competing interests. The authors declare no competing interests.

Ethics approval. Not applicable. The study uses public satellite-derived environmental data and administrative and land-cover layers; it involves no human participants, animals, biological samples, or field permits.

Data and code availability. The data and code supporting the findings of this study are available from the corresponding author upon reasonable request.

Author contributions. Author identities and contribution statements are supplied in the separate non-anonymized file.

Author contributions. C.M.C-R.: conceptualization, proportional spectral formulation, data processing, visualization, writing–original draft. M.M.L-F.: mathematical review, computational review, writing–review and editing. W.C-L.: proportional-calculus review, methodological interpretation, writing–review and editing. All authors approved the final version of the manuscript.

Use of artificial-intelligence tools. A language model assisted with language editing, document organization, and LaTeX preparation. It was not credited as an author. The authors checked all data processing, numerical outputs, citations, interpretations, and final wording and retain full responsibility for the manuscript.

References

Allen RG, Pereira LS, Raes D, Smith M (1998) Crop evapotranspiration: Guidelines for computing crop water requirements. FAO Irrigation and Drainage Paper 56. Food and Agriculture Organization of the United Nations, Rome. https://www.fao.org/4/x0490e/x0490e00.htm

Bashirov AE, Kurpinar EM, Ozyapici A (2008) Multiplicative calculus and its applications. Journal of Mathematical Analysis and Applications 337:36–48. https://doi.org/10.1016/j.jmaa.2007.03.081

Blatchford ML, Mannaerts CM, Njuki SM, Nouri H, Zeng Y, Pelgrum H, Wonink S, Karimi P (2020) Evaluation of WaPOR V2 evapotranspiration products across Africa. Hydrological Processes 34:3200–3221. https://doi.org/10.1002/hyp.13791

Burgin M, Czachor M (2020) Non-Diophantine Arithmetics in Mathematics, Physics and Psychology. World Scientific, Singapore. https://doi.org/10.1142/11665

Butzer PL, Jansche S (1997) A direct approach to the Mellin transform. Journal of Fourier Analysis and Applications 3:325–376. https://doi.org/10.1007/BF02649101

Campillay-Llanos W, Guevara F, Pinto M, Torres R (2021) Differential and integral proportional calculus: How to find a primitive for a Gaussian-type function. International Journal of Mathematical Education in Science and Technology 52:463–476. https://doi.org/10.1080/0020739X.2020.1763489

Czachor M (2020) Unifying aspects of generalized calculus. Entropy 22:1180. https://doi.org/10.3390/e22101180

ESA WorldCover Consortium (2026) ESA WorldCover 10 m 2021 v200. Google Earth Engine Data Catalog. Accessed 1 August 2026. https://developers.google.com/earth-engine/datasets/catalog/ESA_WorldCover_v200

FAO (2018) WaPOR Database Methodology: Level 1. Remote Sensing for Water Productivity Technical Report: Methodology Series. Food and Agriculture Organization of the United Nations, Rome. https://www.fao.org/3/i7315en/i7315en.pdf

FAO (2025) WaPOR version 3 now available in Google Earth Engine. Food and Agriculture Organization of the United Nations. https://www.fao.org/in-action/remote-sensing-for-water-productivity/news-and-events/news/news-detail/wapor-v3-data-now-available-on-the-google-earth-engine-data-catalogue/en

FAO GAUL (2026) Global Administrative Unit Layers 2015, first-level administrative units. Google Earth Engine Data Catalog. Accessed 1 August 2026. https://developers.google.com/earth-engine/datasets/catalog/FAO_GAUL_2015_level1

FAO WaPOR (2026) WaPOR Actual Evapotranspiration and Interception 3.0, Level 1 dekadal product. Google Earth Engine Data Catalog. Accessed 1 August 2026. https://developers.google.com/earth-engine/datasets/catalog/FAO_WAPOR_3_L1_AETI_D

Folland GB (1995) A Course in Abstract Harmonic Analysis. CRC Press, Boca Raton. ISBN 9780849384905.

Google Earth Engine (2026) Resampling and reducing resolution. Google for Developers. Accessed 1 August 2026. https://developers.google.com/earth-engine/guides/resample

Grossman M, Katz R (1972) Non-Newtonian Calculus: A Self-Contained, Elementary Exposition of the Authors' Investigations. Lee Press, Pigeon Cove, Massachusetts.

OpenStreetMap contributors (2026) OpenStreetMap data and copyright. Accessed 1 August 2026. https://www.openstreetmap.org/copyright

Pinto M, Torres R, Campillay-Llanos W, Guevara-Morales F (2020) Applications of proportional calculus and a non-Newtonian logistic growth model. Proyecciones 39:1471–1513. https://doi.org/10.22199/issn.0717-6279-2020-06-0090

Zanaga D, Van De Kerchove R, Daems D, De Keersmaecker W, Brockmann C, Kirches G, Wevers J, Cartus O, Santoro M, Fritz S, Lesiv M, Herold M, Tsendbazar NE, Xu P, Ramoino F, Arino O (2022) ESA WorldCover 10 m 2021 v200. Zenodo. https://doi.org/10.5281/zenodo.7254221